Krzysztof KULIKOWSKI[1], Andrzej SIKORSKI[2]

Bialystok University of Technology (1), (2)

Comparison of new DPC methods for two- and three-level AC/DC converters

Abstract. *The paper briefly describes and compares some new methods of Direct Power Control of a two- and three-level AC/DC converter. The basis for comparing the methods was the equality of switching energy losses in each of the methods.*

Streszczenie. *Artykuł zwięźle opisuje, oraz porównuje nowe metody bezpośredniej regulacji mocy dwu- i trójpoziomowego przekształtnika AC/DC współpracującego z siecią. Podstawą porównania metod była równość strat na przełączanie dla każdej z metod. (**Porównanie nowych metod bezpośredniej regulacji mocy dwu- i trójpoziomowych przekształtników AC/DC**)*

Keywords: DPC, three-level AC/DC inverter.
Słowa kluczowe: DPC, trójpoziomowy przekształtnik AC/DC.

Introduction

In order to demonstrate the advantages of the application of more expensive solutions i.e. a 3-level converter in comparison with a 2-level one, a mere comparison of both structures using basic methods seems to be inadequate. New modified methods of direct power control [1],[2],[3],[4] of an AC/DC converter eliminate some disadvantages of DPC method [5],[6] and also reduce the frequency of switchings for the same values of current deformation coefficients. This paper presents a brief description and comparison of modified methods of vector control of 2- and 3-level AC/DC converters.

Mathematical model of converter

The relationships (1) and (2) [7] describe the input voltage vectors of the converter in αβ stationary reference frame with respect to three- and two-level configuration [8].

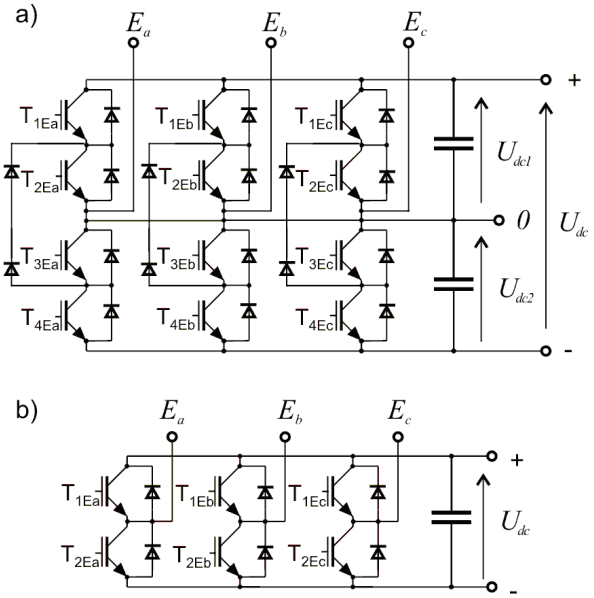

Fig.1. Configuration of three-level (a) and two-level (b)converter

$$(1)\qquad \boldsymbol{U}_d[n]=\begin{cases}\frac{2}{3}U_{dc}\cdot e^{j(n-21)\frac{\pi}{3}}, \text{ for } n=\{21,22...,26\}\\ \frac{\sqrt{3}}{3}U_{dc}\cdot e^{j(n-15)\frac{\pi}{3}}, \text{ for } n=\{15,16...,20\}\\ \frac{1}{3}U_{dc}\cdot e^{j(n-3)\frac{\pi}{3}}, \text{ for } n=\{3,4,...,14\}\\ \textbf{"0"}, \text{ for } n=\{0,1,2\}\end{cases}$$

$$(2)\qquad \boldsymbol{U}_d[n]=\begin{cases}\frac{2}{3}U_{dc}\cdot e^{j(n-1)\frac{\pi}{3}}, dla\ n=\{1,2...,6\}\\ \textbf{"0"}, dla\ n=\{0,7\}\end{cases}$$

where: U_{dc} – DC link voltage, n = 0,1,2... , ***"0"*** – zero vector, n – vector number.

Vectors of current derivative of AC/DC converter

The AC/DC converter showed in Fig. 2 can be described by relationship (2) in αβ stationary reference frame and relationship (3) in xy rotating reference frame.

$$(3)\qquad \boldsymbol{E}\cdot e^{j\omega_1 t}=L\frac{d}{dt}\boldsymbol{i}_{\alpha\beta}+\boldsymbol{U}_d[n]$$

$$(4)\qquad \boldsymbol{E}=L\frac{d}{dt}\boldsymbol{i}_{xy}+j\omega_1\boldsymbol{i}_{xy}+\boldsymbol{U}_d[n]\cdot e^{-j\omega_1 t}$$

where: $\boldsymbol{i}_{\alpha\beta}$ – vector of current in αβ stationary reference frame, $\boldsymbol{i}_{xy}$ - vector of current in xy rotating reference frame, L - inductance of network reactor, $\boldsymbol{E}$ - vector of net voltage.

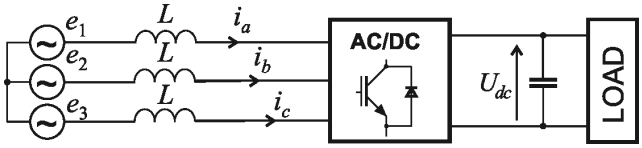

Fig.2. Schematic diagram of AC/DC converter

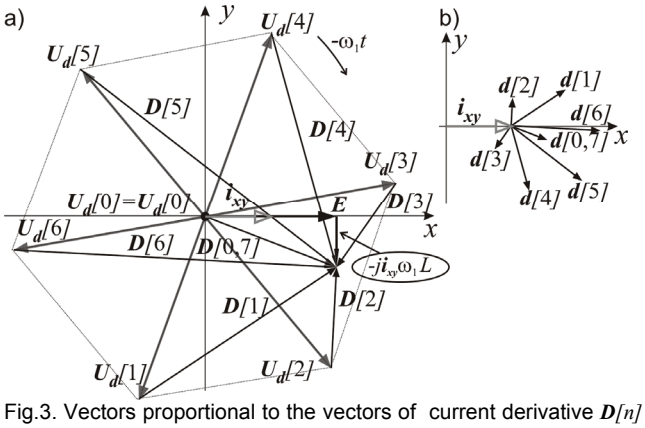

Fig.3. Vectors proportional to the vectors of current derivative $\boldsymbol{D}[n]$ (a), and vectors of current derivative $\boldsymbol{d}[n]$ (b)

Dependences (5) and (6) of the above vectors are described by transformation equation (4). The obtained vectors of current derivatives determine the direction and speed of current changes depending on the voltage vectors of the converter [9].

$$\boldsymbol{D}[n] = L\frac{d}{dt}\boldsymbol{i}_{xy} = E - j\omega_1 L\boldsymbol{i}_{xy} - \boldsymbol{U}_d[n]\cdot e^{-j\omega_1 t} \tag{5}$$

$$\boldsymbol{d}[n] = \frac{d}{dt}\boldsymbol{i}_{xy} = \frac{1}{L}\boldsymbol{D}[n] \tag{6}$$

where: $\boldsymbol{D}[n]$ - vectors proportional to the vectors of current derivative, $\boldsymbol{d}[n]$ - vectors of current derivative.

DPC method

The DPC [5],[6] similarly to the DTC [10] method makes it possible to control both current vector components by selecting voltage vector $\boldsymbol{U_d}[n]$ from the voltage vector selection table. The choice depends on sector N as well as the current comparator states. The selection of sector N is determined by the vector angle of virtual flux. The DPC method assumes that the virtual flux is delayed with respect to the vector of net voltage $\boldsymbol{E}$ by approximately π/2.

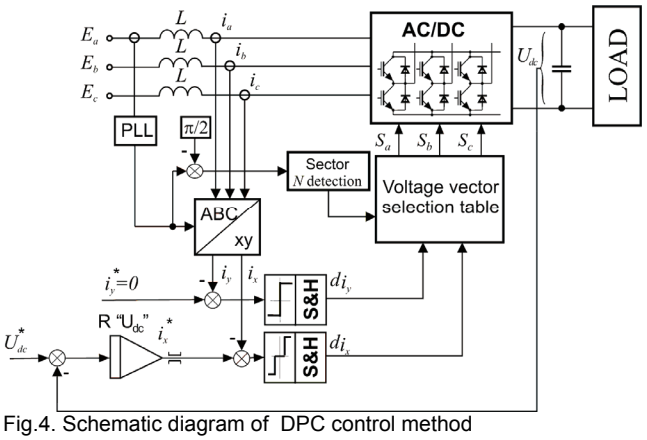

Fig.4. Schematic diagram of DPC control method

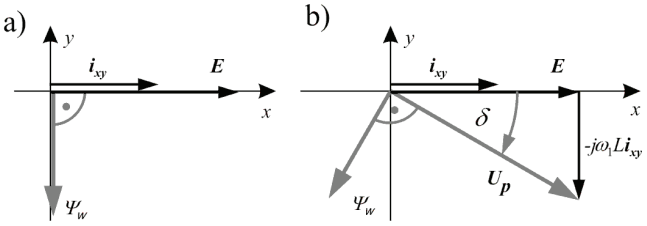

Fig.5. Graphic interpretation of the vector of virtual flux in DPC (a) and DPC-δ (b) control method

DPC 3x2-δ method

The DPC-3x2 method does not to take into account the voltage drop caused by the passage of current through the network reactor, which results in voltage shift on the converter feeder clamps with respect to the vector of net voltage $\boldsymbol{E}$ by angle δ. It also has a larger amplitude (see Fig. 5). The shift between these voltage vectors may also bring about an incorrect sector selection and, in consequence, deteriorate the quality of control. To minimize this negative effect we introduce a converter input voltage vector described by formula (7), to take over the control process [11].

$$\boldsymbol{U_p} = \boldsymbol{E} - j\omega_1 L\boldsymbol{i_{xy}} \tag{7}$$

where: $\boldsymbol{U_p}$ – converter input voltage vector

By introducing the notion of the converter input voltage vector, dependence (5) takes the shape of (8).

$$\boldsymbol{D}[n] = L\frac{d}{dt}\boldsymbol{i_{xy}} = \boldsymbol{U_p} - \boldsymbol{U_d}[n]\cdot e^{-j\omega_1 t} \tag{8}$$

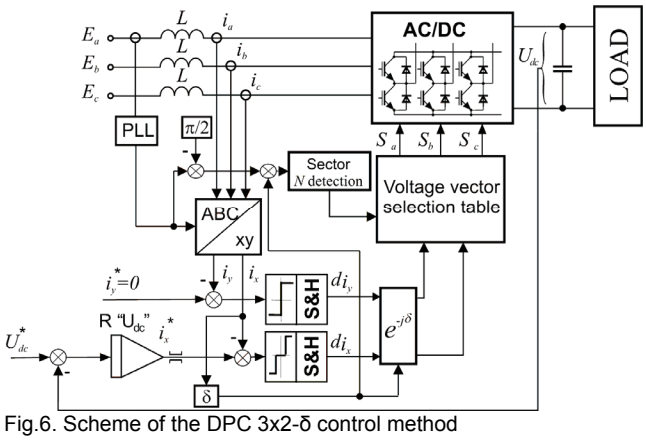

Fig.6. Scheme of the DPC 3x2-δ control method

To adjust the control in relation to $\boldsymbol{U_p}$, voltage vector of virtual flux should be turned by angle δ and the current errors in the xy rotating reference frame - by angle $-\delta$ respectively. Finally, the control structure of the DPC-3x2-δ will take the shape introduced in Fig. 6.

Assuming that $i_y \approx 0$, the angle between vectors of voltages $\boldsymbol{E}$ and $\boldsymbol{U_p}$ (Fig. 5) can be described by dependence (9) [9].

$$\delta = -arctg\left(\frac{\omega L i_x}{|\boldsymbol{E}|}\right) \tag{9}$$

Table 1. Voltage vector selection table for DPC 3x2-δ method

		N=1	N=2	N=3	N=4	N=5	N=6
		vector number (n)					
d_y= 1	d_x= 1	6	1	2	3	4	5
	d_x= 0	1	2	3	4	5	6
	d_x= -1	2	3	4	5	6	1
d_y= -1	d_x= 1	5	6	1	2	3	4
	d_x= 0	4	5	6	1	2	3
	d_x= -1	3	4	5	6	1	2

DPC 5x2-δ method

The DPC 5x2-δ [11] algorithm is , in fact, the DPC 3x2-δ method supplemented by the use of the three-level converter capabilities. The schematic diagram of the method is shown in Fig. 7.

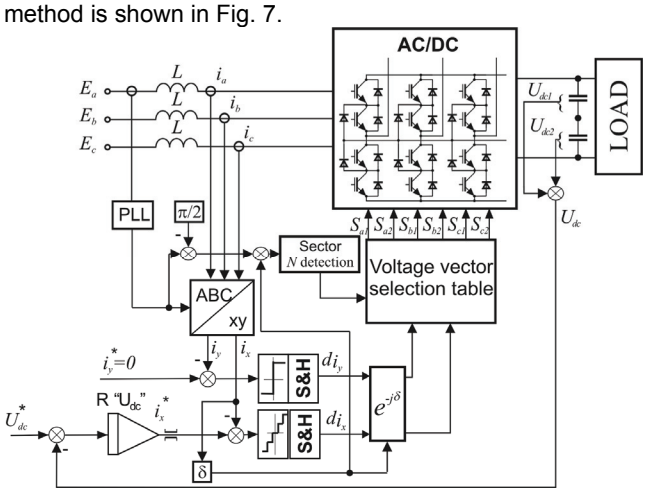

Fig.7. Scheme of the DPC 5x2-δ control method

Due to an increased number of available voltage vectors, the number of current comparator levels in axis x rose from 3 to 5. Additional current comparator levels are used to control current by means of short current and long current derivatives in the static and dynamic state respectively.

Table 2. voltage vector selection table for DPC 5x2-δ method

		N= 1	N= 2	N= 3	N= 4	N= 5	N= 6
		vector number (n)					
d_y= 1	d_x= 2	26	21	22	23	24	25
	d_x= 1	8,14	3,9	4,10	5,11	6,12	7,13
	d_x= 0	3,9	4,10	5,11	6,12	7,13	8,14
	d_x= -1	4,10	5,11	6,12	7,13	8,14	3,9
	d_x= -2	22	23	24	25	26	21
d_y= -1	d_x= 2	25	26	21	22	23	24
	d_x= 1	7,13	8,14	3,9	4,10	5,11	6,12
	d_x= 0	6,12	7,13	8,14	3,9	4,10	5,11
	d_x= -1	5,11	6,12	7,13	8,14	3,9	4,10
	d_x= -2	23	24	25	26	21	22

DPC-3A

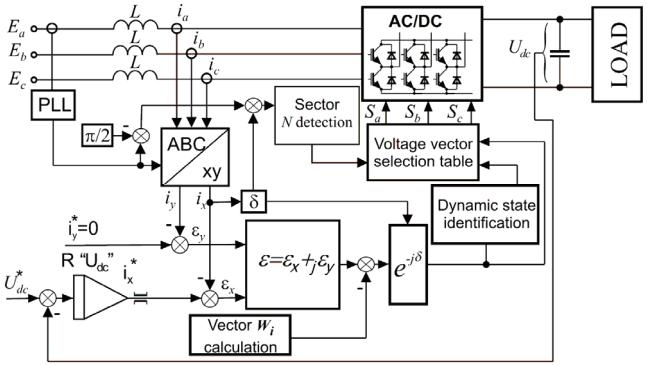

Fig.8. Schematic diagram of DPC-3A method

The DPC-3A [3] method is a modification of DPC 3x2-δ analogous to that of DTC-3A. The purpose of this modification is to decrease the switching frequency with similar deformation coefficients of phase currents.

As shown in [10], the division of the error area in the DPC method is not optimal. The determination of the optimal boundary requires a delimitation of such a dividing line, where the impact of the two adjacent voltage vectors are equivalent. The DPC-3A method has been devised to optimize the division of the error area.

It was shown [10] that the boundaries of a optimum error distribution area are made up of three half-lines of common origin, and turned against each other by 120º. The boundaries of error distribution area are shifted by angle δ with respect to the x-axis and the common origin of boundaries are shifted from the origin of the coordinate system by $\boldsymbol{W_i}$ vector (Fig. 10).

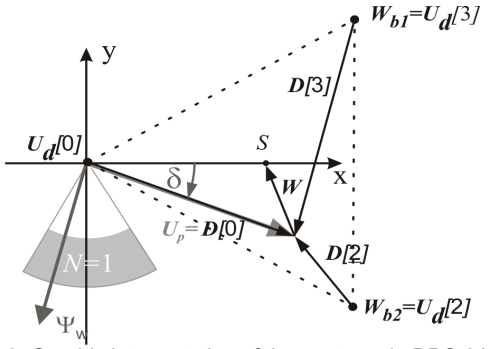

Fig.9. Graphic interpretation of the vector $\boldsymbol{W}$ in DPC-3A method

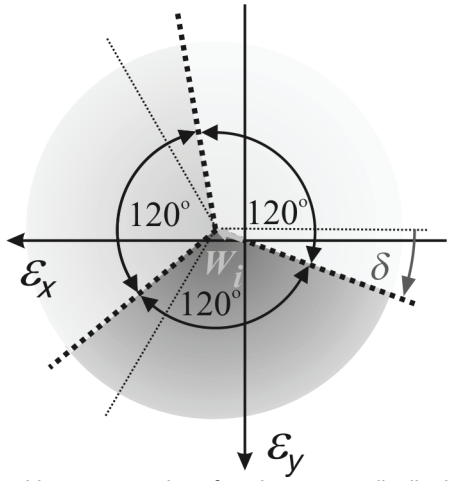

Fig.10. Graphic representation of optimum error distribution area

As each operation of turning and shifting of the whole error area would be troublesome, it can be replaced by an inverse operation performed on the error vector, i.e. shifting it by vector $-\boldsymbol{W_i}$ and turning by angle $-\delta$ (Fig. 11).

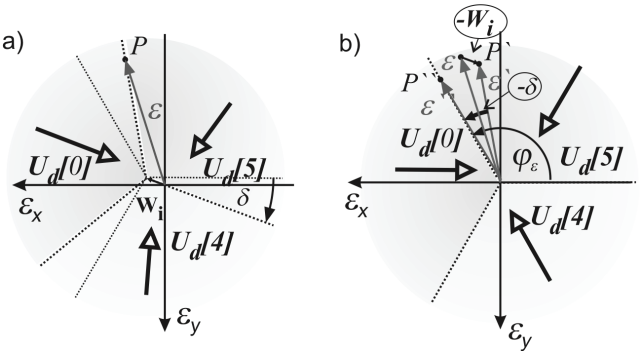

Fig.11. Graphic representation of the equivalence operation of the turn by angle δ and shift by vector $\boldsymbol{W_i}$ made on the error area (a) and the shift by vector $-\boldsymbol{W_i}$ and turn by angle $-\delta$ of the error vector (b)

$\boldsymbol{W_i}$ vector is proportional to voltage vector $\boldsymbol{W}$ that constitutes the difference between voltage vector $\boldsymbol{U_p}$ and the centre of delta composed of three voltage vectors ($\boldsymbol{W_{b1}}$, $\boldsymbol{W_{b2}}$, **"0"**).

In DPC-3A method the real value of current is compared to set values of current in both axes of rotating reference frame. Error vector ε is thus created from ε_x,ε_y and subsequently transformed as shown in Fig. 11b, i.e. vector $\boldsymbol{W_i}$ is subtracted from error vector ε and then turned by angle $-\delta$ [10].

$$\boldsymbol{\varepsilon}'' = (\boldsymbol{\varepsilon} - \boldsymbol{W_i}) \cdot e^{-j\delta} = \left|\boldsymbol{\varepsilon}''\right| \cdot e^{j\varphi_\varepsilon} \tag{10}$$

Vector $\boldsymbol{W_i}$ is related to vector by formula (11) [10].

$$\boldsymbol{W_i} = \frac{\boldsymbol{W}}{L} T_p \tag{11}$$

where: T_p – sampling time.

$\boldsymbol{W}$ vector is calculated using formula (12) as shown in Fig. 9.

$$\boldsymbol{W} = \boldsymbol{S} - \boldsymbol{U_p} \tag{12}$$

where $\boldsymbol{S}$ is the vector of the centre of the equilateral delta built of three voltage vectors characterized by the shortest current derivatives in actual N sector.

Vector $\boldsymbol{S}$ can be calculated using formula (13) [10].

$$\boldsymbol{S} = \frac{1}{3}(\boldsymbol{W_{b1}}e^{j\delta} + \boldsymbol{W_{b2}}e^{j\delta}) \tag{13}$$

where: $\boldsymbol{W_{b1}}$, $\boldsymbol{W_{b2}}$ – currently used voltage vectors $\boldsymbol{U_d[n]}$ (Fig. 9)

Table 3. voltage vector selection table for DPC-3A method

	N= 1	N= 2	N= 3	N= 4	N= 5	N= 6
φ_ε	vector number (n)					
(0,2π/3)	3	4	5	6	1	2
(2π/3, 4π/3)	0 (7)					
(4π/3, 2π)	2	3	4	5	6	1

DPC-3L-3A

The DPC-3L-3Am [12] (Direct Power Control – 3 Level – 3 Area with modifications) method is a modification of DPC-3A method making use of an increased number of active vectors of three –level converter.

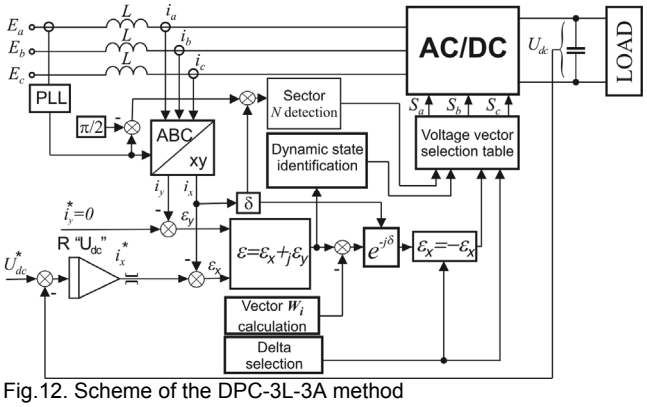

Fig.12. Scheme of the DPC-3L-3A method

In three-level converter each N sector can be divided into four deltas that, in turn, are divided into 3 voltage vectors $\boldsymbol{U_d[n]}$ (Fig. 13). In each of the equilateral triangles formed by the voltage converter an optimal error area (Fig. 14) analogous to of DPC-3A method can be determined.

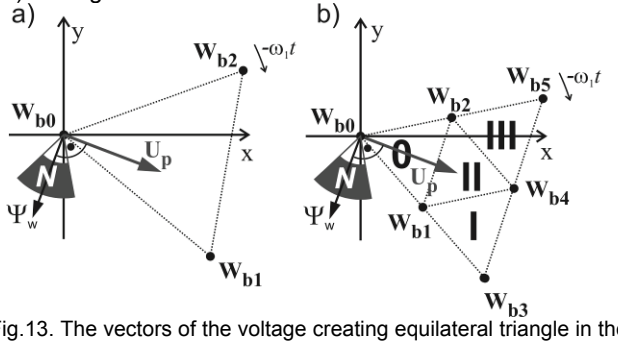

Fig.13. The vectors of the voltage creating equilateral triangle in the sector N = 1 for two-level (a) and three-level (b) converters

As can be seen in Fig. 14, error distribution areas in triangles 0, I, and III are the same. Also the error area in triangle II can by expressed in a similar form, however it requires a change of the sign of component x of the error vector into an opposite one (Fig. 15). Ultimately, DPC-3am control system for the three-level converter takes the form shown in Fig. 12.

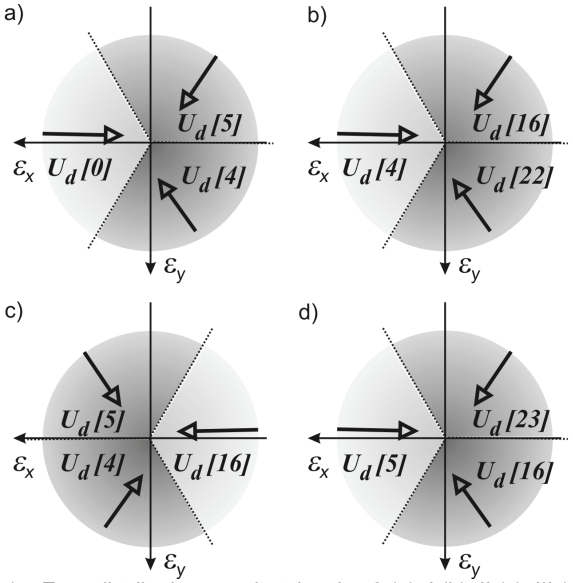

Fig.14. Error distribution area in triangles 0 (a), I (b), II (c), III (d) in sector N = 1

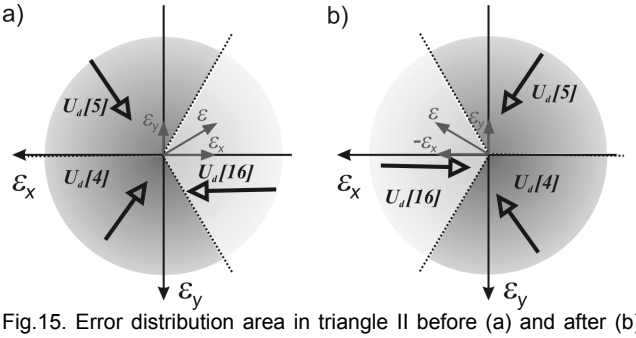

Fig.15. Error distribution area in triangle II before (a) and after (b) the change of the sign of component x of the error vector in sector N = 1

In DPC-3L-3A control method the real value of current is compared to set values of current in both axes of rotating reference frames. Error vector ε is thus created out from errors ε_x,ε_y and subsequently transformed in agreement with formula 14, i.e. vector $\boldsymbol{W_i}$ is subtracted from error vector ε and then turned by angle $-\delta$. In the case when the end of converter input voltage vector $\boldsymbol{U_p}$ is in delta II the sign of component x is changed into the opposite [12].

$$\left|\varepsilon''\right| \cdot e^{j\varphi_\varepsilon} = \begin{cases} (\varepsilon_x + j\varepsilon_y - \boldsymbol{W_i}) \cdot e^{-j\delta}, \text{ for deltas } 0, I, III \\ (-\varepsilon_x + j\varepsilon_y - \boldsymbol{W_i}) \cdot e^{-j\delta}, \text{ for delta } II \end{cases} \tag{14}$$

Vectors $\boldsymbol{W_i}$ and $\boldsymbol{W}$ can be calculated from formulas (11),(12), similarly to DPC-3A method. Vector $\boldsymbol{S}$ is dependent on delta where the converter input voltage vector $\boldsymbol{U_p}$ is currently used. The vector is described by formula (15) [12].

$$S = \begin{cases} 1/3(\boldsymbol{W_{b0}} + \boldsymbol{W_{b1}} + \boldsymbol{W_{b2}}), \text{ for triangle } 0 \\ 1/3(\boldsymbol{W_{b1}} + \boldsymbol{W_{b3}} + \boldsymbol{W_{b4}}), \text{ for triangle } I \\ 1/3(\boldsymbol{W_{b1}} + \boldsymbol{W_{b2}} + \boldsymbol{W_{b4}}), \text{ for triangle } II \\ 1/3(\boldsymbol{W_{b2}} + \boldsymbol{W_{b4}} + \boldsymbol{W_{b5}}), \text{ for triangle } III \end{cases} \tag{15}$$

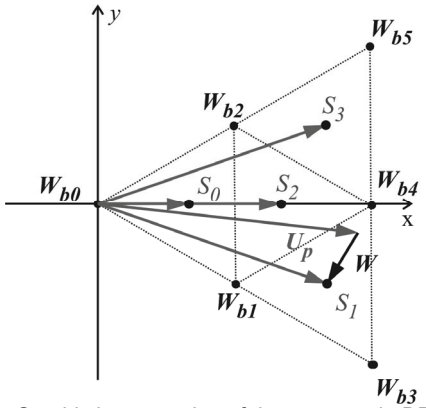

Fig.16. Graphic interpretation of the vector $\boldsymbol{W}$ in DPC-3L-3A control method

Table 4. voltage vector selection table for DPC-3L-3A method

		N= 1	N= 2	N= 3	N= 4	N= 5	N= 6
φ_ε	triangle	vector number (n)					
$\left(0; \frac{2\pi}{3}\right)$	**0**	5,11	6,12	7,13	8,14	3,9	4,10
	I	16	17	18	19	20	15
	II	5,11	6,12	7,13	8,14	3,9	4,10
	III	23	24	25	26	21	22
$\left(\frac{2\pi}{3}, \frac{4\pi}{3}\right)$	**0**	0,1,2	0,1,2	0,1,2	0,1,2	0,1,2	0,1,2
	I	4,10	5,11	6,12	7,13	8,14	3,9
	II	16	17	18	19	20	15
	III	5,11	6,12	7,13	8,14	3,9	4,10
$\left(\frac{4\pi}{3}, 2\pi\right)$	**0**	4,10	5,11	6,12	7,13	8,14	3,9
	I	22	23	24	25	26	21
	II	4,10	5,11	6,12	7,13	8,14	3,9
	III	16	17	18	19	20	15

Comparison of DPC control methods

The simulations were performed in Matlab Simulink environment for two values of DC link voltage i.e. 800 V and 1400 V, and for three set values of current i.e.10, 20 and 30A. The inductance value of network reactors used in the simulation amounted to 20 mH. The basis for comparing the methods in the static state was the similarity of the coefficient of network phase current deformations described by dependence (16). The values determined in simulations performed for DPC 3x2-δ method at 60 kHz switchings were adopted as reference values. To compare the methods coefficients of current deformations in xy rotating reference frame were determined and defined by formulas (17), (18).

$$I_{a(\,puls\,)RMS} = \sqrt{\frac{1}{T_o}\int_0^{T_o}(i_a - i_{a1})^2\,dt} \tag{16}$$

where: $I_{a(puls)RMS}$ – rms value of all current harmonics obtained by subtracting the first harmonic from the actual value of phase current, T_o – net voltage period, i_a – actual value of phase current, i_{a1} – actual value of the first harmonic of phase current.

$$I_{x(\,puls\,)RMS} = \sqrt{\frac{1}{T_o}\int_0^{T_o}(I_x - I_x^*)^2\,dt} \tag{17}$$

$$I_{y(\,puls\,)RMS} = \sqrt{\frac{1}{T_o}\int_0^{T_o}(I_y - I_y^*)^2\,dt} \tag{18}$$

where: $I_{x(puls)RMS}$, $I_{y(puls)RMS}$ – rms values of current components in xy rotating reference frame after subtracting the set values.

Table 5. Results of simulations

Set value / Method	U_{dc}	V	800			1400		
	I^*_x	A	10	20	30	10	20	30
DPC 3x2-δ	$I_{a(puls)RMS}$	A	0,375	0,393	0,369	0,972	0,952	0,983
DPC-5x2-δ		A	0,371	0,391	0,371	0,961	0,901	0,974
DPC-3A		A	0,378	0,391	0,359	0,966	0,941	0,974
DPC-3L3A		A	0,361	0,371	0,349	0,872	0,915	0,915
DPC-3x2-δ	$I_{x(puls)RMS}$	A	0,741	0,560	0,552	1,016	0,975	1,054
DPC-5x2-δ		A	0,366	0,377	0,370	0,856	0,821	1,007
DPC-3A		A	0,343	0,346	0,328	0,849	0,835	0,845
DPC-3L3A		A	0,340	0,357	0,356	0,940	0,951	0,845
DPC-3x2-δ	$I_{y(puls)RMS}$	A	0,456	0,502	0,551	1,200	1,232	1,311
DPC-5x2-δ		A	0,421	0,475	0,501	1,059	1,021	1,116
DPC-3A		A	0,426	0,422	0,379	1,036	1,031	1,079
DPC-3L3A		A	0,383	0,437	0,371	0,794	0,873	0,979
DPC-3x2-δ	f	kHz	60	60	60	60	60	60
DPC-5x2-δ		kHz	82	74	69	74	72	64
DPC-3A		kHz	44	41	41	30	31	35
DPC-3L3A		kHz	22	23	24	11	11	10

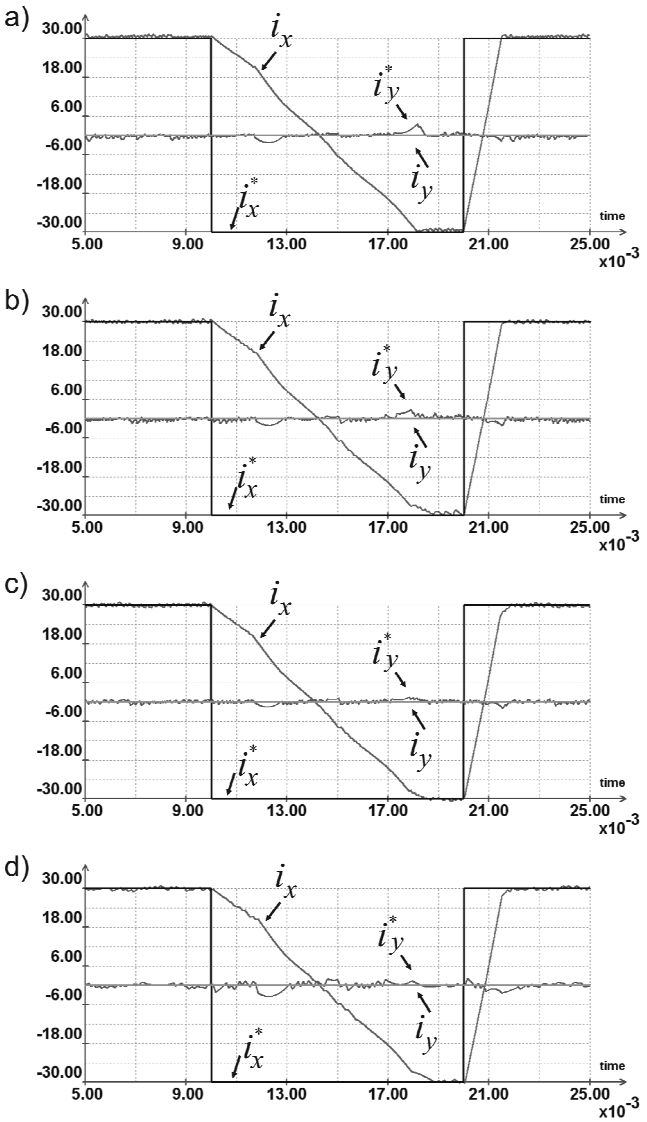

Fig.17. Time courses of current vector components in xy rotating reference frame in the dynamic state for methods: DPC 3x2-δ (a), DPC 5x2-δ (b) DPC-3A (c), DPC-3L-3A (d)

It be should emphasized here that in order to correctly interpret the simulation results, a tree-level converter was used in both DPC 5x2-δ and DPC-3L-3A methods. The

switching of the switching devices in three-level converters occur at twice lower voltage than in two-level ones. As a result, switching energy losses in tree-level converters operating at the same switching frequency is twice smaller.

It follows from Table V that the use of the DPC-3A method reduces the number of two-level converter switchings by approximately 27-50% compared with the DPC 3x2-δ method.

The use of the DPC 5x2-δ method will cause an increase of the number of switchings by about 7-37% when compared to the DPC 3x2-δ method. Keeping in mind that all switchings take place at twice lower voltage, switching energy losses when using this method, in most cases, should be a little lower than with the DPC-3A method.

Basing on the simulation results (see: Table V), we can state that the DPC-3L-3A method is characterized by the lowest switching frequency.

In the dynamic state the methods were compared on the basis of the time courses of current vector components in xy rotating reference frame during step changes of the set value of current component in axis x from 30 A to -30 A (Fig. 17).

All the methods in the dynamic state have shown similar properties. This is due to the fact that each of the presented control methods requires the identification dynamic states where voltage vectors giving the longest current derivatives are selected.

Conclusion

The results of simulations have shown that using new modified methods of Direct Power Control in two- as well three-level converters is more advantageous. In static states, with similar values of current deformations, it is possible to operate converters with lower frequency switchings than in DPC methods for the same converter configuration, thus reducing switching energy losses.

In some applications using two-level converters controlled by the DPC-3A method would be more cost-effective than using more expensive three-level solutions controlled by the DPC 5x2-δ method. It was the DPC-3L-3A method that showed the lowest switching frequency among all the other methods compared.

The dynamics of all the presented control methods is comparable owing to the introduction of the identification of the actual state and the use of voltage vectors giving longer current derivatives.

REFERENCES

[1] G. Escobar, M. F. Martinez-Montejano, R. E. Torres Olguin, A. A. Valdez, An adaptive direct power control for three-phase pwm rectifier in the unbalanced case, *Power Electronics Specialists Conference 2008*, June 2008, 3150-3155.

[2] A. Baktash, A. Vahedi, M. A. S. Masoum, Improved Switching Table For Direct Power Control Of Three-Phase PWM Rectifier, *Australasian Universities Power Engineering Conference 2007*, *Australasian Universities*, December 2007, 1-5.

[3] K. Kulikowski, A. Sikorski, Sterowanie przekształtnika AC/DC współpracującego z siecią metodą DPC-3A, *Przegląd Elektrotechniczny*, 88 (2010), No.4, 130-134.

[4] J. Eloy-Garcia, S. Arnaltes, J. L. Rodriguez-Amenedo, Extended direct power control for multilevel inverters including DC link middle point voltage control, *Electric Power Applications*, No.4, July 2007, 571-580.

[5] S. Vazquez, J. A. Sanchez, J. M. Carrasco, J. I. Leon, E. Galvan, A Model-Based Direct Power Control for Three-Phase Power Converters, *IEEE Transactions on Industrial Electronics* , 55(2008), No. 4, 1647-1657.

[6] M. Malinowski, M. P. Kazmierkowski, S. Hansen, F. Blaabjerg, G.D. Marques, Virtual-flux-based direct power control of three-phase PWM rectifiers, *Industry Applications, IEEE Transactions on* , 37(2001), No. 4, 1019-1027.

[7] M. Korzeniewski, Nowe algorytmy bezpośredniej regulacji momentu i strumienia silnika indukcyjnego zasilanego z trójpoziomowego przekształtnika DC/AC, *Rozprawa Doktorska*, Politechnika Białostocka, Białystok 2009.

[8] B.-R. Lin, T.-Y.Yang, Three-phase AC/DC converter with high power factor, *Electric Power Applications, IEE Proceedings*, 152(2005), No. 3, 757- 764.

[9] A. Sikorski, Problemy minimalizacji strat łączeniowych w przekształtnikach AC/DC/A – PWM zasilających maszynę indukcyjną, *Wydział Wydawnictw i Poligrafii*, Białystok 1998.

[10] A. Sikorski, Bezpośrednia regulacja momentu i strumienia silnika indukcyjnego, *Oficyna Wydawnicza Politechniki Białostockiej*, Białystok 2009.

[11] K. Kulikowski, A. Sikorski, Regulacja mocy trójpoziomowego przekształtnika AC/DC współpracującego z siecią, *Przegląd Elektrotechniczny*, 86 (2010), No. 2, 279-284.

[12] K. Kulikowski, A. Sikorski, Sterowanie trójpoziomowego przekształtnika AC/DC współpracującego z siecią metodą DPC-3L-3Am, *XIII Sympozjum Podstawowe Problemy Energoelektroniki, Elektromechaniki i Mechatroniki 2009*, Polska, Wisła 2009.

***Authors**: mgr inż. Krzysztof Kulikowski, Bialystok University of Technology, Division for Power Electronics and Electric Drivers, ul. Wiejska 45D, 15-351 Białystok, E-mail: k.kulikowski@we.pb.edu.pl; dr hab. inż. Andrzej Sikorski, Bialystok University of Technology, Division for Power Electronics and Electric Drivers, ul. Wiejska 45D, 15-351 Białystok, E-mail: sikorski@pb.edu.pl.*